ACEEE Int. J. on Signal and Image Processing , Vol. 5, No. 1, January 2014

Microelectronic Circuit Analogous to Hydrogen Bonding Network in Active Site of β-lactamase

Rostislav P. Rusev[1], Elitsa E. Gieva[2], George V. Angelov[2], Rossen I. Radonov[2], and Marin H. Hristov[2]
[1] Technical University of Sofia/Department of Technology and Management of Communication Systems, Sofia, Bulgaria
Email: rusev@ecad.tu-sofia.bg
[2] Technical University of Sofia/Department of Microelectronics, Sofia, Bulgaria
Email: {gieva, gva, radonov, mhristov}@ecad.tu-sofia.bg

***Abstract*—A microelectronic circuit of block-elements functionally analogous to two hydrogen bonding networks is investigated. The hydrogen bonding networks are extracted from *â*-lactamase protein and are formed in its active site. Each hydrogen bond of the network is described in equivalent electrical circuit by three or four-terminal block-element. Each block-element is coded in Matlab. Static and dynamic analyses are performed. The resultant microelectronic circuit analogous to the hydrogen bonding network operates as current mirror, sine pulse source, triangular pulse source as well as signal modulator.**

***Index Terms*—Hydrogen bonding network, behavioral modeling, Matlab, Verilog-A, proteins.**

I. Introduction

Bioelectronics is dynamically evolving part of electronics. The integration of biomolecules with electronic elements to yield functional devices attracts substantial research efforts because of the basic fundamental scientific questions and the potential practical applications of the systems. A fundamental requirement of any bioelectronics system is the existence of electronic coupling and communication between the biomolecules and the electronic supports [1]. The understanding of charge transport phenomena through biological matrices attracted in the past decades, and continues to evolve, intensive theoretical and experimental work. The seminal contributions of the Marcus theory [2], the super exchange charge transfer theory [3], and the definition of superior tunneling paths in proteins [4] had a tremendous impact on the understanding of biological processes such as the electron transfer in the photosynthetic reaction center, or the charge transport in redox-proteins that are the key reactions for numerous electrochemical and photoelectrochemical biosensing systems.

The small dimensions of the bioobjects make them appropriate for various types of biosensors [5], pH-sensors [6], light sensors [7], etc. A biosensor is generally defined as an analytical device which converts a biological response into a quantifiable and processable signal. A continuous feedback between elegant experimental work employing structurally engineered proteins and theoretical analysis of the results led to the formulation of a comprehensive paradigm for electron and proton transport in proteins [8].

In our previous research [9, 10, 11, 12, 13] we have investigated information transfer through hydrogen bonding networks of the β-lactamase protein. After extraction of protein hydrogen bonding networks (HBNs) from the enzyme periphery, we have investigated the charge transport. We have matched each residue (from protein HBN) to functionally analogous block-element to describe the proton transfer with polynomials. Next, static and dynamic analyses have been performed on the circuits consisting of block-elements. The simulation results are compared to conventional microelectronic circuits.

In this paper we focus on information transfer via protein hydrogen bonding networks and their operation as analogs to conventional electronic circuits. In particular, we investigate HBNs formed in the active site of the β-lactamase protein.

II. Model and Equations

The two hydrogen bonding networks formed at the active site during the four intermediates of acyl-enzyme reaction are shown in Fig.1; they are denoted “nucleophilic” and “electrophilic”. Proton transfer in each hydrogen bonding network was studied in [14]. In the paper is introduced proton transfer parameter K (in accordance with the constant of the electron transfer). It has dimension of free energy, and from the calculations it can be interpreted as follows: the greater parameter K - so much readily accomplished proton transfer between donor and acceptor from HBNs, i.e. the proton current will be greater. On the other hand the parameter of proton transfer depends on the donor/acceptor potentials similarly to the potentials supplying the microelectronic components. Therefore we can construct three and four-terminal electronic block-elements analogous to the hydrogen bonds.

During the four intermediates of the half-cycle of the acyl-enzyme reaction participate the same residues and water molecules. For this reason the corresponding microelectronic block-elements in the equivalent electrical circuits are the same but they are connected in different way. Therefore, two functionally analogous microelectronic circuits for the four intermediates of acyl-reaction are constructed; the circuits

The research is related to the project No BG051PO001-3.3.06-0046 “Development support of PhD students, postdoctoral researchers and young scientists in the field of virtual engineering and industrial technologies”., corresponding author: Elitsa Gieva

DOI: 01.IJSIP.5.1.1450

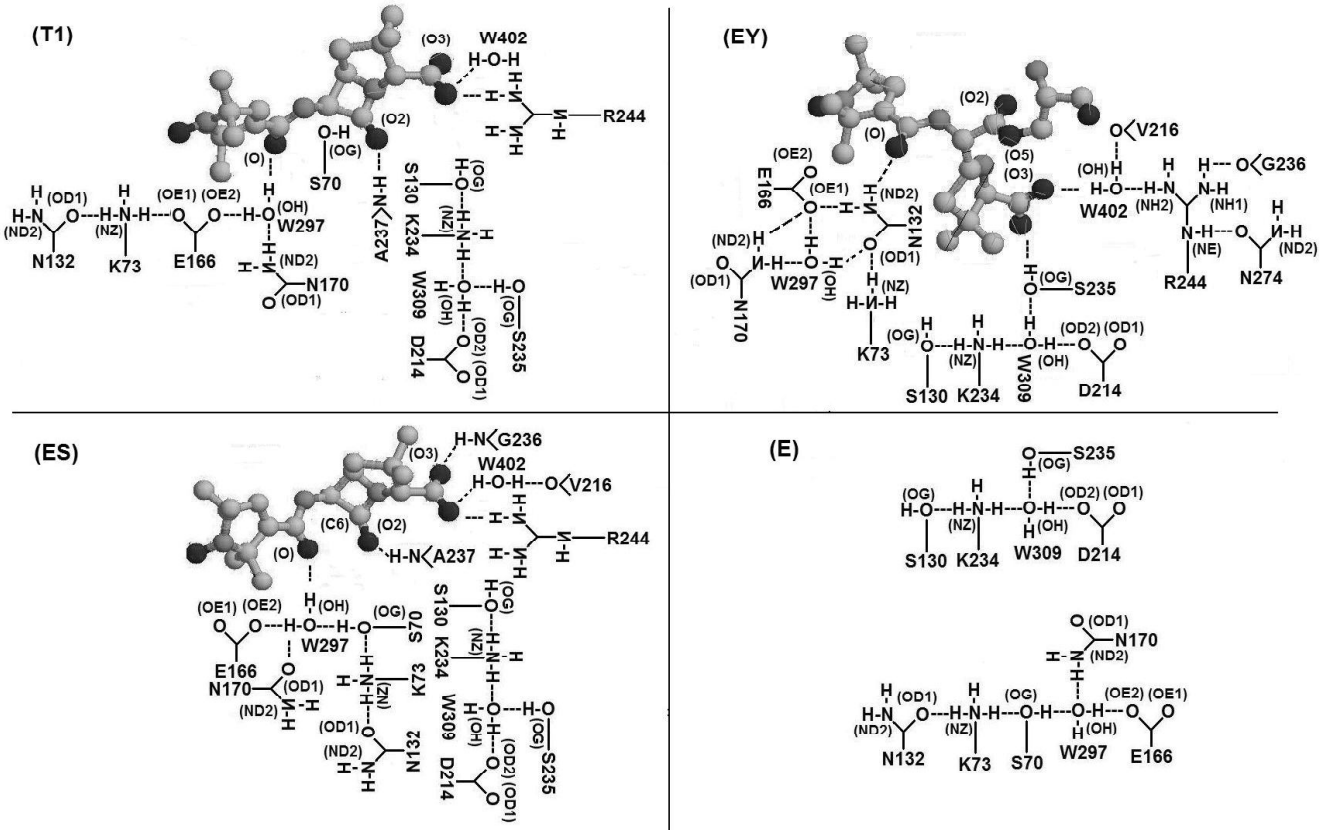

Figure 1. Acyl-enzyme reaction intermediates – HBNs in the active site of: (E) free enzyme, (ES) Michaelis complex, (T1) transient state, (EY) acylenzyme. The first HBN is referred to as "nucleophilic" consists of residue S70, water molecule w297, residues N170, E166, K173, N132 and ligand. The second referred to as "electrophilic" consists of consists of residues S130, K234, water molecule w309, and residues D214, S235

depend on switch S that corresponds to the ligand. In this paper we will analyze one intermediate of the acyl-reaction only, i.e. the free enzyme (state (E) in Fig.1) without a ligand.

In Fig.2 it is shown the microelectronic circuit analogous to HBNs formed in the active site of β–lactamase.

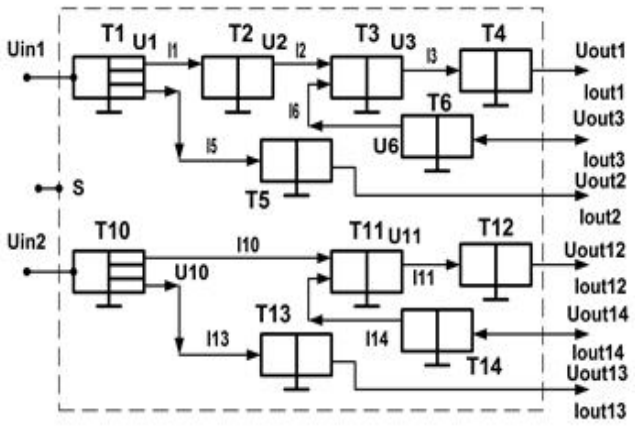

Figure 2. Microelectronic circuit analogous to HBNs formed in the active site of β–lactamase when β–lactamase is free enzyme (state E)

The input voltage of the first electric circuit analogous to "nucleophilic" hydrogen bonding network is labeled as "Uin1". Block-element T1 corresponds to lysine K73NZ. The lysine is a strong proton donor, so in the circuit it is interpreted as a voltage controlled current source. Block-element T2 is juxtaposed to S70OG residue, which is a three terminal block-element with identical input and output voltage and different input and output currents.

In the circuit of Fig. 2 the water molecule w297 is compared to block-element T3. It should be noted that depending on the state of the switch S, block-element T3 changes its function. In this case T3 has two inputs and one output.

The block-element T4 is functionally analogous to E166, which is strong proton acceptor and can form different hydrogen bonds. T4 block-element is represented as a three terminal block-element with one input and one output. The other two block-elements T5 and T6 are similar to asparagines N132 and N170. Asparagine could be both proton-donor and proton-acceptors in the circuit, therefore N132 and N170 can change the direction of the currents as a depending on the switch S.

The input of the second circuit on Fig. 2 is labeled with Uin2. This electrical circuit is functionally analogous to the "electrophilic" hydrogen bonding network, which also has three outputs. Here block-element T10 is also a voltage controlled current source and it corresponds to the strong proton-donor K234NZ. In this block-element (similarly to T1) the two output voltages are identical to the input voltage but the input and output currents are different. The next block-element T11 is analogous to the water molecule w309. In state (E) the element has two inputs and one output. The residue D214 is juxtaposed to block-elements T12; T12 has

DOI: 01.IJSIP.5.1.1450

one input and one output, and the T12 output is also the circuit output. The three terminal block-element T13 is compared to S130OG. Its input and output voltages are identical, but the input-output currents are different. The block-element T14 is the last output block-element of the integrated circuit. It is functionally analogous to S235OG and has the same functions as S130OG (respectively T13).

It should be noted that there is proton transport in both HBNs during the different intermediates of the reaction. The proton transport is influenced by pH and protein-ligand interaction. In this reason, both electrical circuits are not separated from each other (similar to an integrated circuit) and the input voltages of both units are equal in analogy of pH.

The model equations that describe the electrical relations of the each block-element are given below.

Equations (1) and (2) describe the T1 block-element.

$$U_1 = U_{in}; \quad (1)$$

$$I_1 = 3\times10^{-5}U_1^3 - 5\times10^{-5}U_1^2 - 7\times10^{-5}U_1 + 0.0013; \quad (2)$$

Equations (3) and (4) describe the T2 block-element.

$$U_2 = 1.0451\times U_1 - 0.1194; \quad (3)$$

$$I_2 = -0.0236\times U_2^3 + 0.0379\times U_2^2 + 0.124\times U_2 + 1.3046; \quad (4)$$

Equations (5) and (6) describe the T3 block-element.

$$U_3 = 1.0179\times U_2 - 0.039; \quad (5)$$

$$I_3 = 0.0015\times U_3^3 - 0.0015\times U_3^2 - 0.0171\times U_3 + 0.0859; \quad (6)$$

Equations (7) and (8) describe block-element T4.

$$U_4 = 0.9703\times U_3 + 0.0589; \quad (7)$$

$$I_4 = I_3 = I_{out1}; \quad (8)$$

Equations (9) and (10) describe the T5 block-element.

$$U_5 = 0.0457\times U_1^2 + 1.2273\times U_1 - 0.8501; \quad (9)$$

$$I_5 = 0\times U_5 + 0.0001; \quad (10)$$

Equations (11) and (12) describe the T6 block-element.

$$U_6 = 1.0544\times U_3 - 0.0933; \quad (11)$$

$$I_6 = 0.0058\times U_6^2 + 0.0367\times U_6 + 0.7113; \quad (12)$$

Equations (13) and (14) describe the T10 block-element.

$$U_{10} = 0.9701\times U_1 + 0.2072; \quad (13)$$

$$I_{10} = 4\times10^{-5}\times U_{10}^4 - 6\times10^{-5}\times U_{10}^3 - 0.0002\times U_{10}^2 + 0.0004\times U_{10} + 0.00252; \quad (14)$$

Equations (15) and (16) describe the T11 block-element.

$$U_{11} = 0.9835\times U_{10} + 0.1438; \quad (15)$$

$$I_{11} = 2\times10^{-5}\times U_{11}^3 - 13\times10^{-6}\times U_{11}^2 - 0.00015\times U_{11} + 0.00048; \quad (16)$$

Equations (17) and (18) describe the T12 block-element.

$$U_{12} = 0.9683\times U_{11} + 0.458; \quad (17)$$

$$I_{12} = I_{11}; \quad (18)$$

Equations (19) and (20) describe the T13 block-element.

$$U_{13} = 1.1009\times U_{10} - 0.3571; \quad (19)$$

$$I_{13} = 10^{-5}\times U_{13}^4 + 2\times10^{-5}\times U_{13}^3 - 8\times10^{-5}U_{13}^2 + 2\times10^{-5}\times U_{13} + 0.0015; \quad (20)$$

Equations (21) and (22) describe the T14 block-element.

$$U_{14} = 1.034\times U_{11} - 0.1986; \quad (21)$$

$$I_{14} = 0\times U_{14} + 0.0001; \quad (22)$$

The equations are coded in Matlab [15]. Excerpt of the code is given below.

```
U2 = 1.0451*U1 -0.1194;
plot(U1,U2,'linewidth',2);
set(gca,'fontweight','b','fontsize',14)
grid on
title('T2');
xlabel('Uin [V]');
ylabel('U2 [V]');
legend('simulation','data');
set(legend('simulation','data',1),'fontsize',12);
pause;
I2 = - 0.0236*U2.^3 + 0.0379*U2.^2 + 0.124*U2 +1.3046;
load('bsy1_e.dat');
U2exp = bsy1_e(:,3);
I2exp = bsy1_e(:,4);
plot(U2,I2,U2exp,I2exp,'ro','linewidth',2);
set(gca,'fontweight','b','fontsize',14)
grid on
title('T2');
xlabel('U2 [V]');
ylabel('I2 [pA]');
% legend('simulation','data');
set(legend('simulation','data',1),'fontsize',12);
pause;
```

III. Static Analysis

Static analysis is performed in Matlab. First, we tested how well our polynomial *I-V* characteristics describe the components and connections between them. In Fig. 3 are shown the compared results from simulations and the previous data for block elements T1 and T2.

As it can be seen from Fig. 3, the polynomials well describe the functional dependencies of the modeled block elements.

DOI: 01.IJSIP.5.1.1450

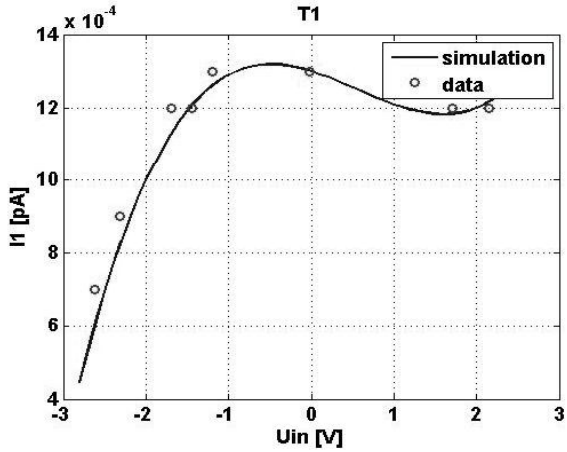

a)

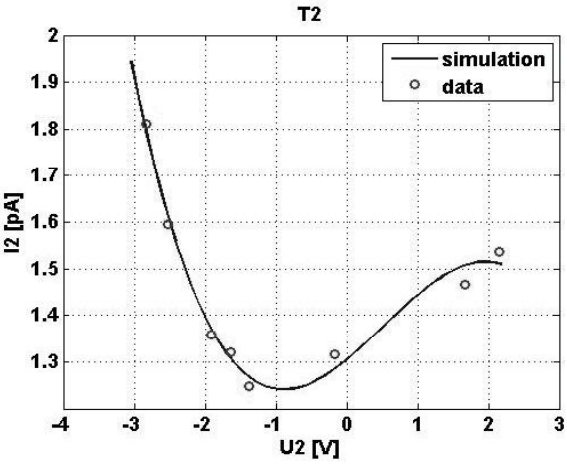

b)

Figure 3. *I-V* characteristic of block elements a) ò1 and b) ò2 (emulating Ê73, S70)

Similar results were seen for the other block elements of the circuit (by this reason they are not shown), and the maximum calculated error is 5.66%.

After the comparative analysis between the simulations and the data taken from [14], a static analysis is made for the entire integrated biocircuit. The results for each output of the circuit are shown below. Fig. 4 shows the *I-V* characteristics of output 1.

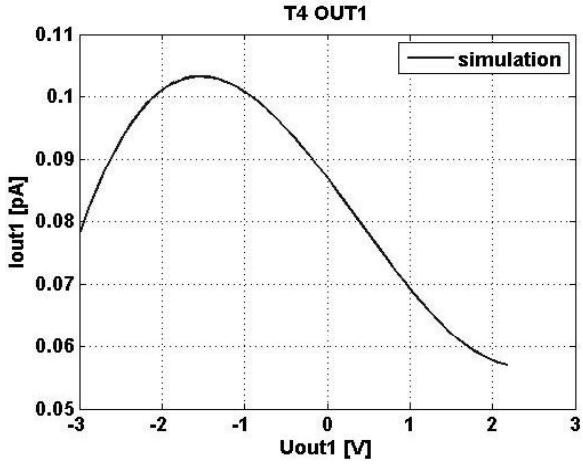

Figure 4. I-V characteristic of first output current

The *I-V* characteristic of first output is similar to *I-V* characteristic of tunnel diode [9].

In Fig. 5 the output voltages are shown.

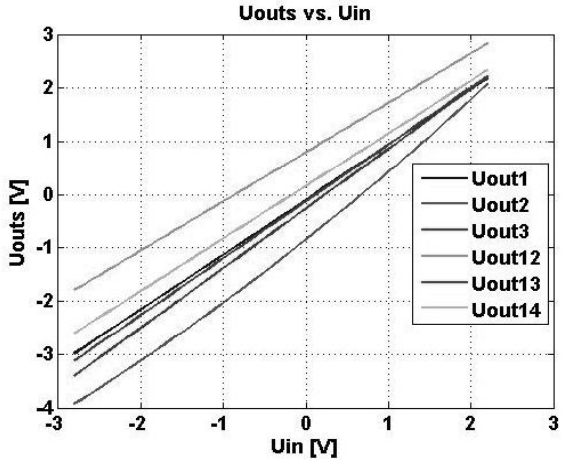

Figure 5. The output voltages vs. input voltage.

The output voltages repeat the form of the input voltage. This is also observed in our previous paper for HBNs in the periphery of β-lactamase protein [9].

In Fig. 6 the current of the second output is shown.

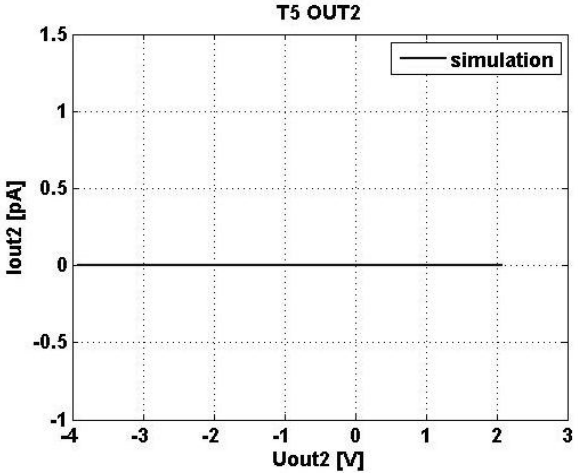

Figure 6. *I-V* characteristic of second output current.

Current does not change with the change of voltage (its value is 0.0001 [pA]). Therefore, this output has characteristics similar to a current source as observed in [10, 11].

In Fig. 7 the current of the third output is shown.

For case E current increases according to an exponential law with increasing voltage and output characteristic is similar to shifted characteristics of diode.

Fig. 8 shows the current characteristic on output 12.

Current is amended by S-shaped law.

At the next output (13) there is a curve which is a combination of the curves of S-shape (Fig. 9).

At the next output 14 (Fig. 10) the current does not change by changing the voltage.

Characteristics are similar to the current generator (Fig. 10), as it was for output 2 [12].

From the standpoint of its mode of use, the circuit could

DOI: 01.IJSIP.5.1.1450

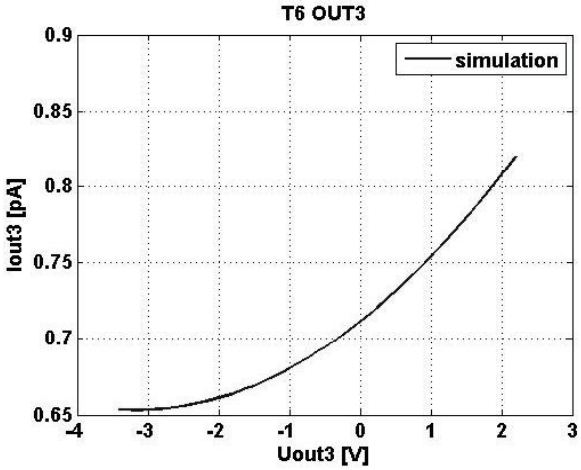

Figure 7. I-V characteristic of third output current

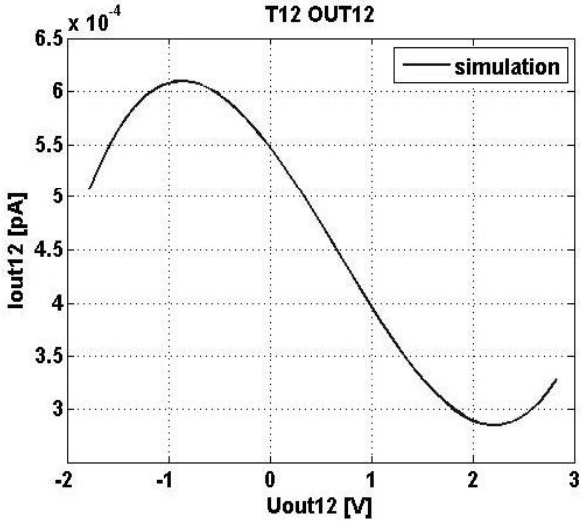

Figure 8. I-V characteristic of twelfth output current

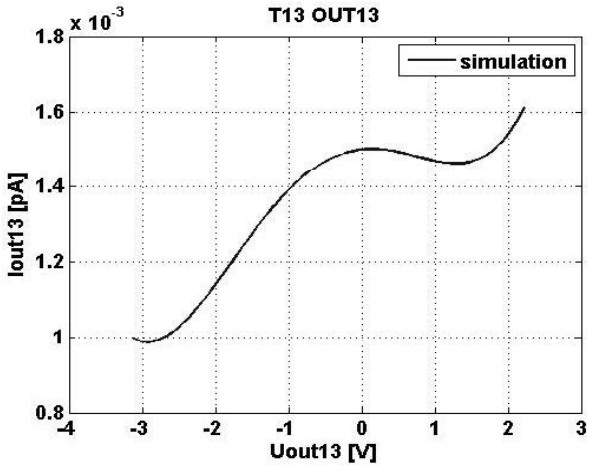

Figure 9. I-V characteristic of thirteenth output current

be used as a current generator or as an amplifier. Further its capabilities will be demonstrated in the dynamic analysis.

IV. Dynamic Analysis

The integrated circuit functionally similar to hydrogen bonding networks in the active site of the protein is a complex

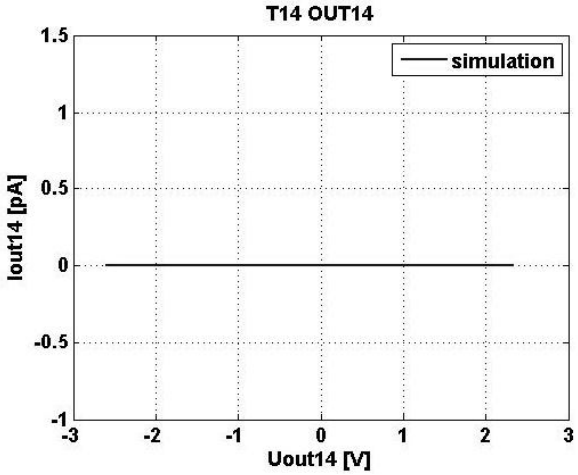

Figure 10. I-V characteristic of fourteenth output current

circuit with multiple output; therefore, a thorough dynamic analysis is required. To understand in detail its mode of action, research were made when applying three types of sinusoidal voltages at the input. First was applied voltage with an amplitude from -2.2 to 2.2 [V] (Fig. 11) and the frequency of 10 [GHz] then was applied voltage with the same frequency, but only the positive or only the negative amplitudes and sweep of 1 [V]. These simulations showed that the output voltage repeats the input voltage in form and frequency, and the amplitude is on the same order.

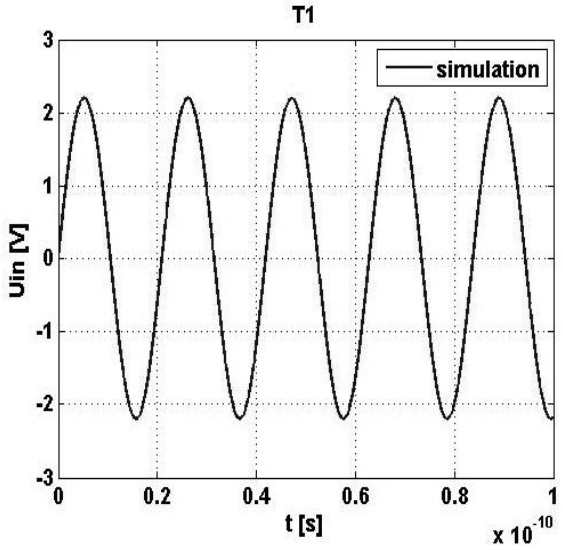

Figure11. The input voltage vs. time Uin = 2.2*sin((5e11)*t)

This behavior was expected because from static analysis we know that the output voltages are shifted off the input voltage by linear law. Therefore, for convenience we will present only the input voltage and output currents vs. time. For output currents again we see that they keep their positive amplitude regardless whether voltages are in negative or positive half-period. As an example, in Fig. 12 we showed voltage and current on output 1, input voltage is with amplitude from -2.2 to +2.2 [V]. If input voltage with positive amplitude is applied (Fig. 13, 14) different signal amplitude sinusoidal signals are generated at output 1; the currents are shifted in relation to the voltages.

DOI: 01.IJSIP.5.1.1450

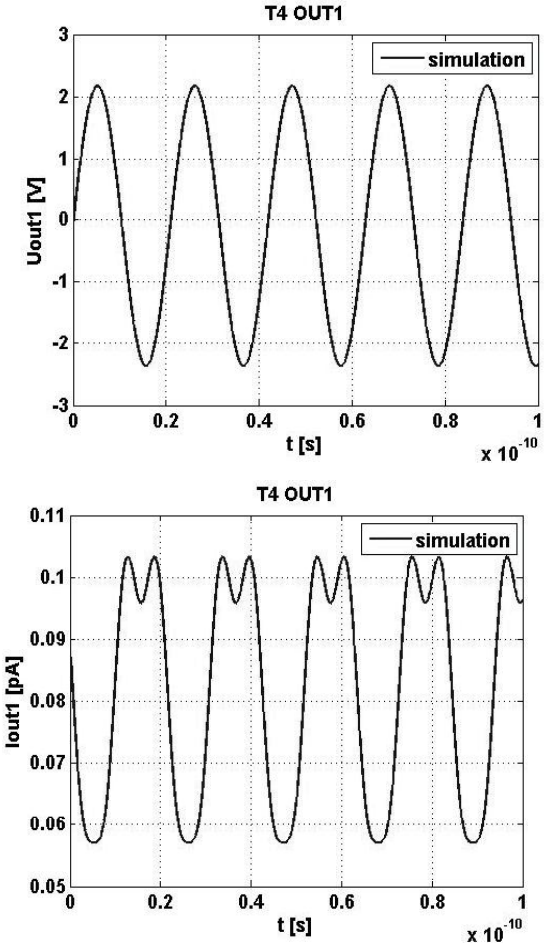

Figure12. The voltage and current on first output vs. time (Uin = 2.2*sin((5e11)*t

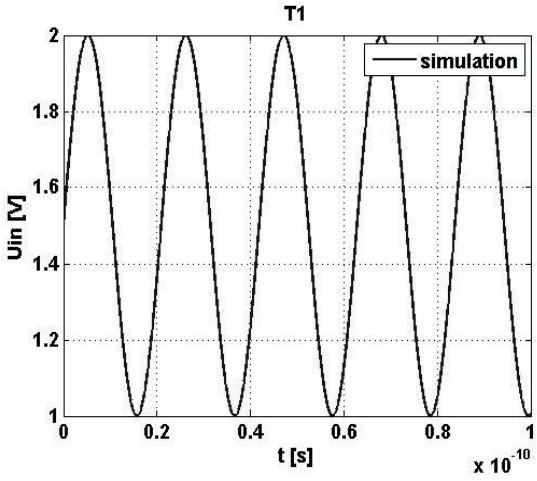

Figure 13. The input voltage vs. time Uin =1,5 +0.5*sin((5e11)*t)

When applied a input voltage with negative amplitude (Fig. 15) for output 1, we obtain the modulated signal with the same phase for current (Fig. 16). Similar phenomena was observed in our previous paper [13].

Simulations show that the second output current does not change (Fig. 17) when applying with different amplitude (and frequency) input voltages.

This output is similar to the output of the current-mirror,

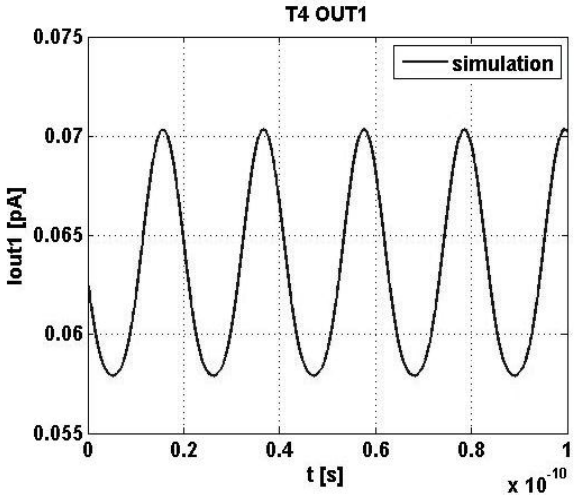

Figure 14. The first output current vs. time (Uin =1,5 +0.5*sin((5e11)*t))

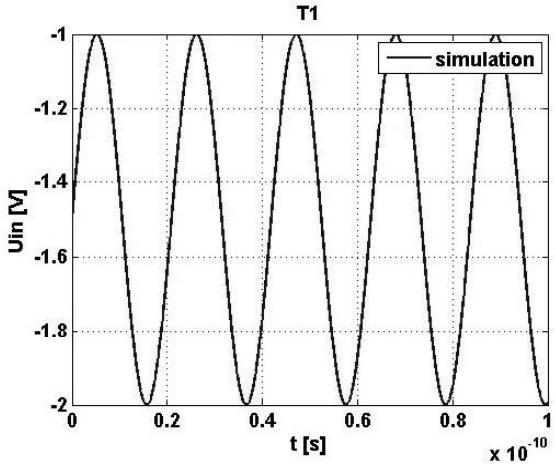

Figure 15. The input voltage vs. time Uin = -1+0.5sin((5e11)*t)

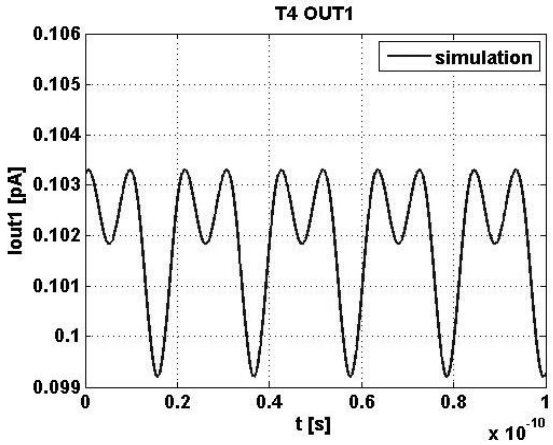

Figure 16. The first output current vs. time Uin = -1+0.5sin((5e11)*t)

i.e. the currents not dependent on a change of the voltage, as determined by the static analysis.

When applying a sinusoidal voltage with a positive amplitude (Fig.15) the output 3 starts to generate sinusoidal signals (Fig. 18).

The same output signals are obtained when applying the

DOI: 01.IJSIP.5.1.1450

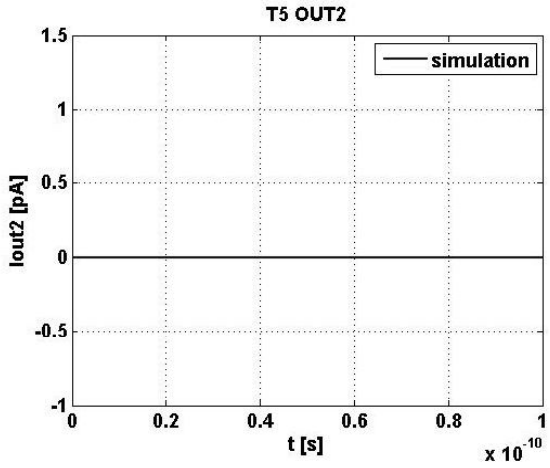

Figure 17. The second output current vs. time

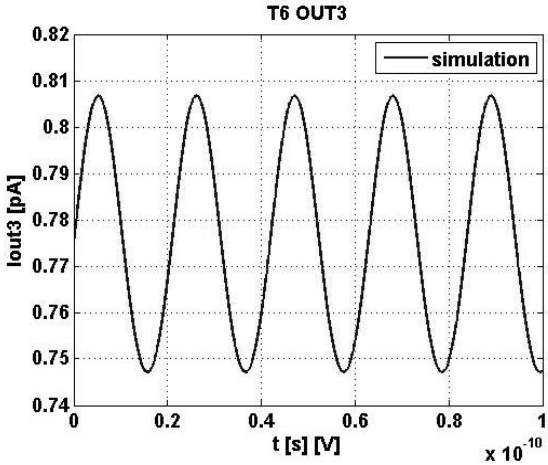

Figure 18. The third output current vs. time (Uin = 1,5 +0.5sin((5e11)*t))

sinusoidal input voltage with negative amplitude. Therefore they are not shown in any figures.

The most complicated generated signals are obtained at the output 12. When is applied a sinusoidal input signal with an amplitude of -2.2 to +2,2 V, then output starts to modulate (Fig. 19).

When applying an input voltages with only positive or only negative amplitude, the circuit allows the generation of other types of signals (triangular) as shown below (Fig. 20).

Generally, only this output of the circuit is able to generate signals, such as number of previously known in electronic devices. These signals can be controlled by changing the amplitude of the input signal.

The situation is similar at output 13 and there is generation of signals with various shape and amplitude depending on the amplitude of the input voltage (Fig. 21, 22). The comparison of the signals at output 13 and output 12 showed that these signals are different.

Output T13 can easily be put into mode that generates sinusoidal signals only. This happens when applying the input voltage with a negative amplitude (Fig. 17).

Here in Fig.22 current is in phase with the input voltage (respectively the output voltages).

The output current at T14 output does not change with

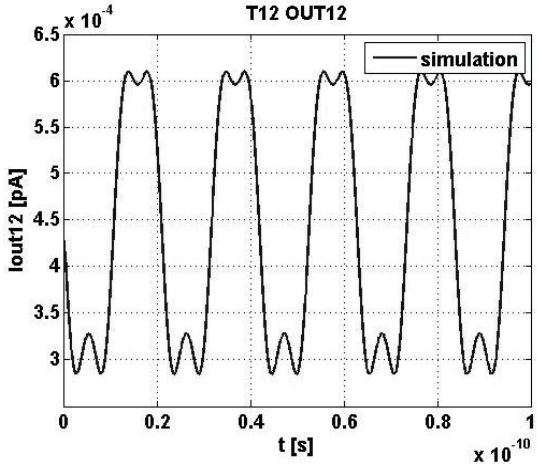

Figure 19. The output current on output 12 vs. time (Uin = 2.2*sin((5e11)*t))

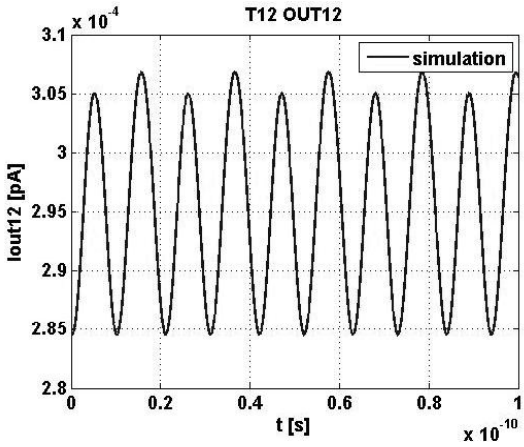

Figure 20. Other types of signals generated on output 12.

the input voltage (Fig. 23): the currents are constant (0.0001 [pA]) and the output behaves similarly to the current-mirror or current source.

The results of the dynamic analysis showed that the integrated circuit functionally analogous to the hydrogen bonding network in the active site of the protein β-lactamase could operate in different modes and to generate different types of signals and can also modulate the different in amplitude and shape signals.

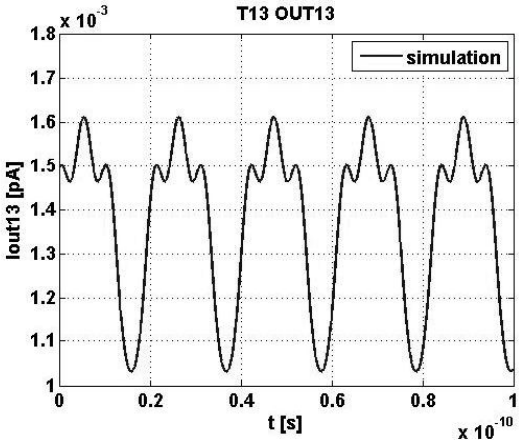

Figure 21. The output current on output 13 vs. time (Uin = 2.2*sin((5e11)*t))

DOI: 01.IJSIP.5.1.1450

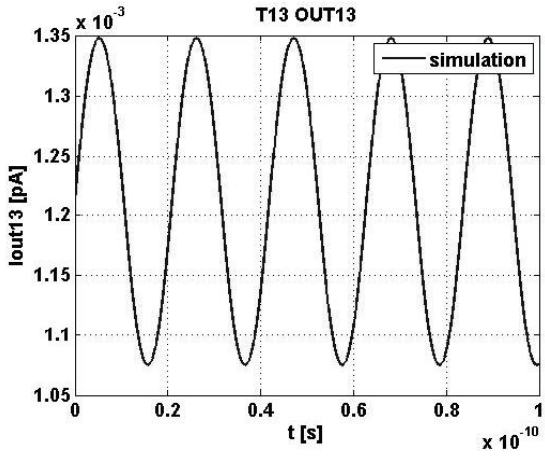

Figure 22. The input voltage and output current on output 13 vs. time (Uin = -1.5 +0.5sin((5e11)*t))

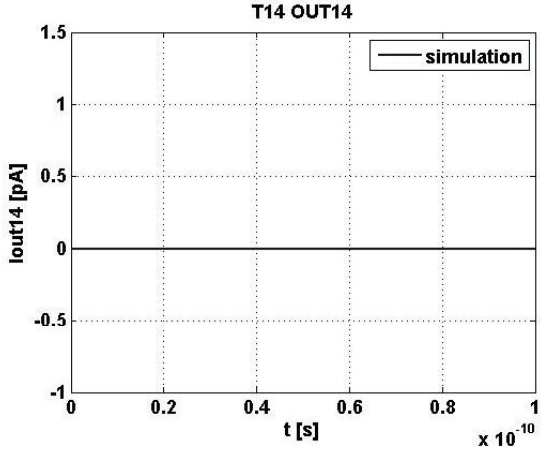

Figure 23. The output current on output 14 vs. time (Uin = 2.2*sin((5e11)*t))

V. Conclusion

The block-elements of the microelectronic circuit well describe the behavior of the hydrogen bonding network. Static analysis shows that the circuit could operate as tunnel diode, current source and multifunctional device. From the results of the dynamic analysis, it can be seen that the circuit could operate in different modes and generate in their outputs different types of signals. The circuit has functions similar to current-mirror, source of different signals with sinusoidal and triangular amplitude, and can modulate signals with different amplitude and shape. The results obtained prove that the modeled circuit can emulate the behavior of hydrogen bonding networks for microelectronics applications.

Acknowledgment

The research is related to the project No BG051PO001-3.3.06-0046 “Development support of PhD students, postdoctoral researchers and young scientists in the field of virtual engineering and industrial technologies”. The project is implemented with the financial support of the Operational Programme Human Resources Development, co-financed by the European Union through the European Social Fund.

References

[1] Prof. Dr. Itamar Willner and Dr. Eugenii Katz, Bioelectronics – An Introduction (pages 1–13), Online ISBN: 9783527603763, DOI: 10.1002/352760376X, Copyright © 2005 Wiley-VCH Verlag GmbH & Co. KGaA

[2] A. Markus, and V. Helms, “Compact parameter set for fast estimation of proton transfer rates”, J. Phys. Chem, Vol. 114, pp. 3, 2001.

[3] Bixon, M.; Jortner, J. “Electron Transfer – from Isolated Molecules to Biomolecules”. Adv. Chem. Phys. 1999, 106, 35-202.

[4] H.B. Gray, J.R. Winkler, Electron tunneling through proteins, Q. Rev. Biophys. 36 (2003) 341–372.

[5] Prof. Dr. Itamar Willner, Dr. Eugenii Katz, Bioelectronics: From Theory to Applications, Chapter 12, Published Online: 23 MAY 2005, DOI:10.1002/352760376X.ch12.

[6] Paola Fabbri, Francesco Pilati, Luigi Rovati, Ruel McKenzie, Jovan Mijovic, Optical Materials, Poly(ethylene oxide)–silica hybrids entrapping sensitive dyes for biomedical optical pH sensors: Molecular dynamics and optical response, Optical Materials 33 (2011) 1362–1369, 2011.

[7] Sudarshan Rajagopal and Keith Moffat, Crystal structure of a photoactive yellow protein from a sensor histidine kinase: Conformational variability and signal transduction, 1649-1654 (2002)

[8] H. B. Gray and J. R. Winkler, “Electron Transfer in Proteins”, Annu. Rev. Biochem. 1996, 65, 537-561.

[9] Gieva, Elitsa E., Characterization of a Hydrogen Bonding Network in Cadence using Verilog-A, E+E Journal – pp 18-24, ‘3-4’ 2012

[10] Elitsa Gieva, Rostislav Rusev, George Angelov, Marin Hristov, Tihomir Takov, Internation Journal BIOAUTOMATION, 2012, 16(4), pp 291-308, Published: January 8, 2013

[11] Rostislav Rusev, George Angelov, Elitsa Gieva, Marin Hristov, and Tihomir Takov, Hydrogen Bonding Network Emulating Frequency Driven Source of Triangular Pulses”, International Journal of Microelectronics and Computer Science, vol.1, No3, pp.291-296, 2010

[12] Elitsa Gieva, R. Rusev, G. Angelov, T. Takov, M. Hristov, “Simulation of Branching Hydrogen Bonding Network in Cadence”, Proc. of the 1st Intl. Conf. Systems, Power, Control, Robotics (SCOPORO ’12), pp. 171-176, Singapore City, Singapore, May 11-13, 2012. ISBN: 978-1-61804-094-7

[13] Elitsa Gieva, Penov L., Rusev R., Angelov G., Hristov M., “Protein Hydrogen Bonding Network Electrical Model and Simulation in Verilog-A”, Annual Journal of ELECTRONICS, Volume 5, Number 2 pp.132-135, ISSN 1313-1842, Sozopol 14-16 September, 2011

[14] Rostislav Rusev, George Angelov, Elitsa Gieva, Boris Atanasov, Marin Hristov, Microelectronic Aspects of Hydrogen Bond Characteristics in Active Site of b-lactamase during the Acylenzyme Reaction, Annual Journal of ELECTRONICS, ISSN 1314-0078, Volume 6 , Number 2 , pp.35-38, 2012.

[15] Matlab website http://www.mathworks.com.

DOI: 01.IJSIP.5.1.1450